Volume 2, Number 2, 2009. pp. 113-123

Jordan Journal of Physics

ARTICLE

Multistream Instability in Two and Three−Species Plasmas

M. S. Bawa'aneh[a], **G. Assayed**[a], **M. Shatnawi**[a], **G. Alna'washi**[a] and **S. Al−Awfi**[b]

[a]*Department of Physics, The Hashemite University, Zarka, Jordan.*
[b]*Department of Physics, Faculty of Science, Taibah University, Madina, Saudi Arabia.*

Received on: 3/12/2008; Accepted on: 16/4/2009

Abstract: A detailed parametric investigation of the linear dispersion relation of electron−ion (e−i) and electron−electron−ion (e−e−i) in the hydrogen plasma fluid is carried out in order to determine the different current driven instabilities that can exist in each case. Equations governing the two−stream (e−i) and three−stream (e−e−i) instabilities in cold plasmas are solved numerically and solutions are thoroughly investigated. For the two−stream instability, numerical solutions of the corresponding dispersion relation show the appearance of an unstable mode for $kv_e > 0$, where k is the wave number and v_e is the electron drift speed. Results reported in some references in literature on the peak value of the instability growth rate, when compared with the numerical result, have been found to overestimate the instability maximum growth rate by 17%, while others' estimates coincide with our numerically obtained value. A three−stream instability regime, with two oppositely drifting electron streams with respect to a static ion stream, is also studied; the presence of the third stream has been found to modify the mode spectra by giving rise to a highly unstable mode compared to that observed in the two−stream case. By increasing the number of electrons in the third stream (and keeping a zero net current in the plasma), a red shift in the instability peak value of the growth rate has been observed with an insignificant change in its peak value.

Keywords: Multistream instabilities; Three-species plasma; Kinetic theory.

Introduction

Instabilities which are dependent on the shape of the velocity distribution function are called velocity−space instabilities or micro-instabilities [1, 2]. One example of velocity space instabilities that occur in plasmas is the two−stream instability [3-7], where two interpenetrating streams of a charged particle fluid with different parallel or antiparallel velocities are in many situations unstable.

Heating of plasma with a high−current relativistic electron beam makes essential use of the plasma return current induced by the beam [8]. From overall energy conservation it is concluded that a large fraction of the beam energy is converted into plasma thermal energy. For reasonable parameters the heating occurs through ion sound turbulence generated by the plasma return current.

Stabilization of the two−stream instability in weakly ionized plasma (equatorial electro-jet) has been studied by Sato [9] using fluid equations. It is shown that a macroscopic quasi-linear process acts to reduce the electron flow to a threshold level (ion sound speed), thereby stabilizing the plasma. This result gives an explanation for constant Doppler shifts of radar echoes in the electro-jet. It is further shown that the saturation level of the fluctuations agrees with that of observations.

Corresponding Author: M. S. Bawa'aneh. **Email**: msb@hu.edu.jo.

A source of growth of the plasma micro-instability is the change in the free energy density W_0 associated with the relative drifts of the plasma components. Current in plasma is a common source of free energy that leads to an increase in instabilities [10]. It has been pointed out by Hirosa [11] that the linear growth of the instability breaks down when the field energy is of the order of $(m_e / m_i)^{2/3} W_0$ and concluded that the anomalous resistivity associated with the instability scales as $(m_e / m_i)^{2/3}$, rather than $(m_e / m_i)^{1/3}$, where m_e and m_i are the electron and ion masses, respectively.

Instabilities that are driven by electron−ion relative drift in two−species Maxwellian plasmas are classified as acoustic instabilities. Such instabilities are most appropriately called two−stream instabilities in case of very high relative drifts (above some characteristic thermal speed) where modes become fluid−like [10]. Also, instabilities are two−stream for zero temperature limits of Maxwellian plasmas where zero−order distribution functions of different species become similar to those shown in Eqs. 3 and 4. S. P. Gary [10] showed instabilities for the two−stream Maxwellian plasma. His results are very similar to dispersion curves obtained for cold plasma especially for plasmas with relative drift velocities larger than thermal velocities. Such extreme situations occur in some regimes (for example in space plasmas [5, 10]). In such regimes, some waves and instabilities have properties that are essentially independent of axial magnetic fields and are charge neutral and bear no steady−state electric fields. So, it is appropriate to investigate the instability of such regimes in non-magnetized quasi-neutral plasmas. Such modes, called ion acoustic−like fluctuations which are essentially electrostatic, are observed in many space plasma contexts such as the solar wind [12, 13, 14] and the earth's bow shock [15].

Ion-electron two-stream instability has been observed experimentally in high intensity accelerators and storage rings [16, 17]. Theoretical studies suggest that the relative streaming motion of the high-intensity particle beam through a background of charged particles provides the free energy to drive the two-stream instability [18, 19]. A background population of electrons can result by secondary emission when energetic beam particles strike the beam-pipe wall. At low energies and for high charge states the beam can very effectively ionize the residual gas. These secondary electrons can be trapped in the beam electrostatic potential in which electrons can accumulate up to a certain saturation level. Above a certain threshold the accumulated electrons induce two-stream-like instabilities in long bunches [18, 22].

V. Lapuerta and E. Ahedo have done extensive work on two−stream instability (see for example [23, 24, 25]) and on multi−stream instability (see for example [26]). The parametric regions where different types of such instabilities dominate as well as relationship between different instabilities are not very well understood and are being studied. For example, the evolution of the ion−acoustic to Buneman instabilities was studied in ref [24].

The study of multi-stream instabilities is, also, of great interest in beam physics [27, 31]. Ronald C. Davidson and Hong Qin investigated the wall−impedance driven collective instability in intense bunched particle beams using the linearized Vlasov equation [27]. The study included a wide variety of applications ranging from the Harris−like instability driven by large temperature anisotropy to the dipole mode two−stream instability of an intense ion beam propagating through an electron background. Detailed stability properties were determined for dipole−mode perturbations for small axial momentum spread of the beam and for cold beam distribution function in the axial direction, a case that corresponds to the largest instability growth rate. R. Bosch investigated the suppression of two−stream hose instabilities at wavelengths shorter than the transverse length of the beam [28]. Calculations showed stabilization of the two−stream instability when the instability wavelength becomes smaller than the transverse beam length. The same suppression has been observed when a proton beam propagates through a channel that consists of electrons and positive ions.

In recent years, quantum effects have been proven to play an important rule in multi-stream instabilities [32, 37]. Haas *et al*. [32] derived a dispersion relation for the one and two-stream instability by using nonlinear Schrödinger-Poisson system to describe the dynamics of the cold plasma. Anderson *et al*. [33] considered a statistical multi-stream description to prove that a Landau-like damping suppresses the two-stream instability. Ali *et al*. [34, 35] derived a general dielectric constant for a magnetized dusty plasma and finally Haijun *et al*. [36, 37] used quantum hydrodynamic equations to derive a general dispersion relation for one and two-stream plasma.

The main objective of this work is to fill a gap in the detailed investigation of the general dispersion relation of the case of the three−stream instability. Numerical calculations presented in this paper for streaming instability in a cold, collision-less plasma account for two and three particle species. In case of three species we have one ion and two electron species. The ratio of the electrons of the second species to the total number of electrons is given by the ratio number *r*. The first electron species drifts with a velocity of v_{1e} with respect to the ion species, while the second electron species has a drift velocity of v_{2e} with respect to ions. The magnitude of v_{2e} is estimated such that the plasma is quasi-neutral, i.e. the net current is zero, which yields a second electron species drifting opposite to the first one. In section 2, model equations will be presented and applied to the case of two streams. In section 3, the nonlinear dispersion relation for the case of three−stream systems will be derived and solved numerically. In section 4, results and conclusions are given.

Two – Stream Instability

A stream of energetic electrons passing through cold plasma can excite ion waves which will grow rapidly in magnitude at the expense of the kinetic energy of the electrons. In cold, uniform and un-magnetized plasmas, where ions are stationary, electrons have a constant drift velocity *v* in a reference frame moving with the ion stream. In collision-less non-magnetized plasmas in which the electrostatic approximation is valid so that the fluctuating fields are described by Poisson's equation, the longitudinal dielectric function ($\varepsilon(k,\omega)$) for multi-species plasmas is given by [10, 31, 32]

$$\varepsilon(k,\omega) = 1 + \sum_j \chi_j(k,\omega), \tag{1}$$

$$\chi_j(k,\omega) = \frac{q_j^2}{m_j \varepsilon_0} \int_{-\infty}^{\infty} \frac{f_{0j}(v)}{(\omega - kv)^2} dv \tag{2}$$

where ε_0 is the electric permittivity for vacuum, χ_j is the electric susceptibility of the j^{th} species of the plasma, ω and *k* are the frequency and wave number of a specified plasma mode, q_j, m_j are the single particle charge and mass, respectively and the function $f_{0j}(v)$ is the equilibrium velocity distribution function of the j^{th} plasma species.

Consider a static ion species, where ions are taken as an immobile neutralizing background of positive charges, and an electron species that drifts with a relative velocity of v_e with respect to the ions. The equilibrium distribution function for the cold ions is given by

$$f_{0i}(v) = n_{0i}\delta(v), \tag{3}$$

where n_{0i} is the equilibrium ion density. Equilibrium distribution function for the electron species drifting with v_e with respect to ions is given by

$$f_{0e}(v) = n_{0e}\delta(v - v_e), \tag{4}$$

where n_{0e} is the equilibrium electron density. The equilibrium distribution functions considered here are obtained from the zero temperature limit of the Maxwellian distribution function that best describes the individual plasma components with no in-homogeneity or anisotropy in the distribution, namely,

$$\left.\begin{aligned} f(v) &= \frac{n_{oj}}{(2\pi)^{3/2} V_j^3} \exp\left(\frac{-v_j^2}{2V_j^2}\right), \\ V_j^2 &= \frac{k_B T_j}{m_j} \end{aligned}\right\} \tag{5}$$

Substituting for the distribution functions from Eqs. 3 and 4 and using Eq. 2, the plasma dielectric function of Eq.1 becomes

$$\varepsilon(k,\omega) = 1 - \omega_{pe}^2 \left[\frac{Zm_e / m_i}{\omega^2} + \frac{1}{(\omega - kv_e)^2} \right] \quad (6)$$

where $n_{0e} = Zn_{0i}$ is used, Z is the single ion charge state and ω_{pe} is the electron plasma frequency. Eq.6 is solved numerically for ω as a function of the wave number k for $\varepsilon(k,\omega) = 0$ that yields the dispersion properties of the plasma. The number of roots of $\varepsilon(k,\omega)$ for given plasma is determined by the choice of the equilibrium distribution function as well as the number of species considered. For a Maxwellian plasma, $\varepsilon(k,\omega)$ has, in general, an infinite number of roots. Most of such modes are acoustic−like ($\omega_r / k \sim const.$), where ω_r is the real part of the frequency [10]. Usually, the instability (the imaginary part of the frequency) of different modes is of most interest.

In this section we obtain a numerical solution for the fourth order dispersion relation of the two stream instability in hydrogen plasma with an emphasis on the unstable modes. All figures shown represent the real and/or imaginary parts of the mode frequency ω normalized to ω_{pe}, versus the wave number k normalized to ω_{pe} / v_e, where v_e represents the electron drift velocity with respect to ions.

Eq. 6 has four roots; the full solution for this equation is shown in Fig. 1, where it is obvious from the equation that ignoring the electron drift would leave us with the two real roots $\omega = \pm\omega_{pe}$, which are the two roots starting in Fig. 1 with ± 1 at $kv_e = 0$. This can be verified analytically using Eq.6. Since ω_{pi} is much smaller than ω_{pe}, the solutions of Eq. 6 in the limit of vanishing ion plasma frequency are $\omega = \pm\omega_{pe} + kv_e$. At *k=0*, both solutions starts at +1 and -1. With increasing k both are shifted upward. This confirms qualitatively the numerical results.

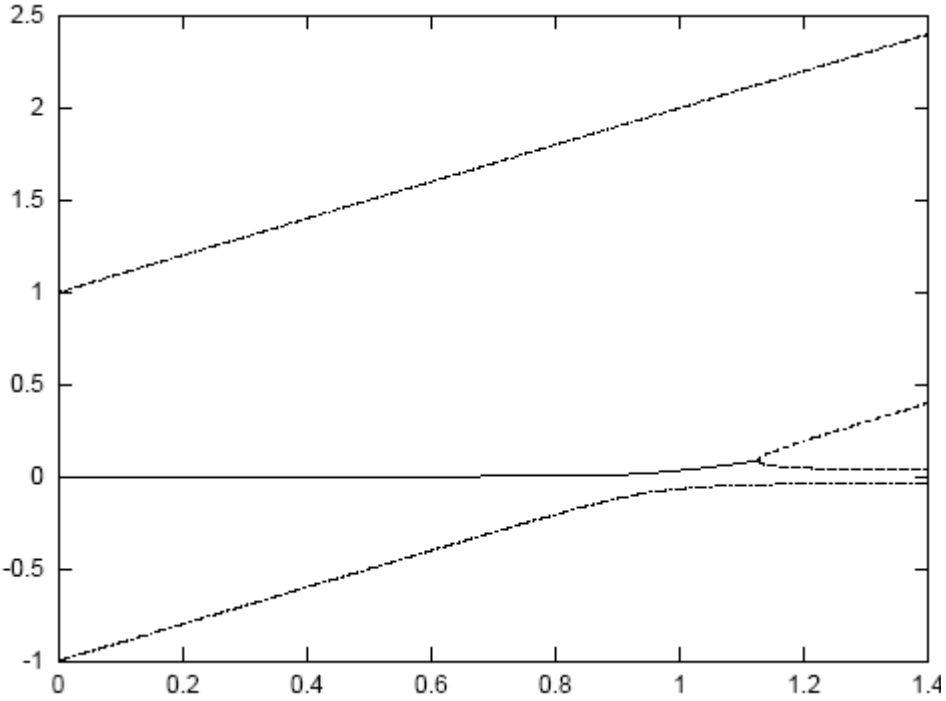

FIG. 1. Real part of the four root solution of Eq.6. Solid line represents two unstable complex conjugate roots. Other lines correspond to real roots.

The presence of the electron drift results in the deviation these two roots as shown in the figure. Also, the presence of the electron drift has given rise to a complex root and its complex conjugate presented in Fig. 1 with the solid line. These unstable roots appear for $kv_e \in (0,1.12)$, beyond which these complex roots disappear and two new real roots appear maintaining a four−root solution for Eq. 6. The unstable root of Fig. 1 (solid line) is plotted in more detail in Fig. 2 together with its imaginary part shown in dashed line. The instability peaks at $kv_e = \omega_{pe}$ as expected, with $\gamma \approx 0.055\omega_{pe}$, dropping after that to a cut−off wavelength, at $kv_e = 1.12\omega_{pe}$. Here, we can compare the value of the growth rate at $kv_e = \omega_{pe}$, where the instability is maximum, with that known in literature; In ref. [31, 32], the maximum value is given by

$$\frac{\gamma}{\omega_{pe}} \approx \left(0.5\frac{m_e}{m_i}\right)^{1/3} \Leftrightarrow \gamma \approx 0.065\omega_{pe}, \qquad (7)$$

while that in ref. [27] is given by

$$\frac{\gamma}{\omega_{pe}} \approx \left(\frac{3\sqrt{3}}{16}\frac{m_e}{m_i}\right)^{1/3} \Leftrightarrow \gamma \approx 0.056\omega_{pe} \qquad (8)$$

From Fig. 2, the numerical value of the maximum growth rate is about $0.055\omega_{pe}$, which agrees with that maximum value shown in ref. [23] and shows an error of 17% in the formulae obtained in ref. [38, 39]. A similar mode was observed in ref. [10] for hot plasmas.

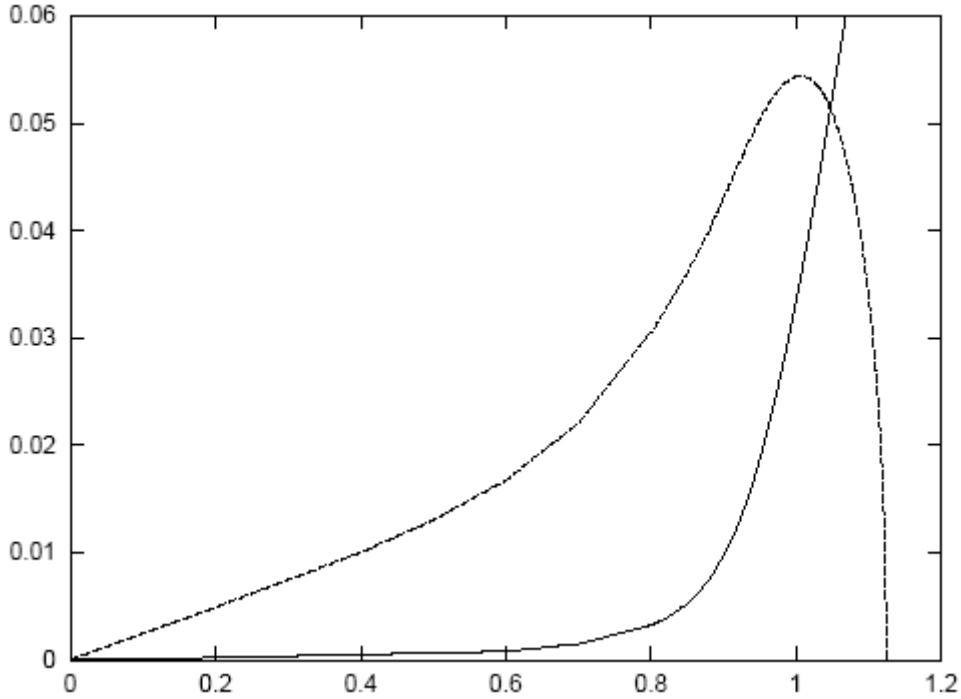

FIG. 2. Real (solid line) and imaginary (dashed line) parts of the frequency versus wave number of the unstable mode for two stream instability.

Three−Stream Instability

In case of three−streams, we consider a system of one ion species and two electron species that drift, relative to ions, with two different speeds given by v_{1e} and v_{2e} in opposite directions. In this case the ion distribution function is still given by Eq.3, while the electron distribution function is given by

$$f_{0e}(v) = n_{0e}\begin{bmatrix}(1-r)\delta(v-v_{1e})\\ +r\delta(v+v_{2e})\end{bmatrix} \qquad (9)$$

where r is the ratio of the number of electrons drifting with speed v_{2e} to the total number of electrons. Substituting the values of the distribution functions for the three species from Eqs. 3 and 9 in Eqs. 1 and 2, the dielectric function of the three−stream plasma becomes,

$$\varepsilon(k,\omega) = 1 - \omega_{pe}^2 \left[\frac{Zm_e / m_i}{\omega^2} + \frac{1-r}{(\omega - kv_{1e})^2} + \frac{r}{(\omega + kv_{2e})^2} \right] \quad (10)$$

Note that Eq. 6 for the two−stream case can be obtained from Eq. 10 simply by setting the ratio number r to zero. For $\varepsilon(k,\omega) = 0$, Eq. 10 is solved numerically for ω as a function of the wave number k using different values of ratio r. The speed v_{2e} is estimated relative to v_{1e} such that the net electric current is zero just to keep the quasi-neutrality of the plasma [10].

The configuration of the electron drifts shows two opposite Doppler shifts in the mode frequencies, namely, $\omega_{1,2} = \omega \pm kv_{e1,2}$. To investigate the instability of the three−stream system, we investigate the roots of the sixth order dispersion relation. Four of the six roots are those obtained in the two−stream case, namely roots shown in Fig. 1, and 2 new complex conjugate roots are, also, obtained. Fig. 3 shows the real part of the two additional complex conjugate roots for the three r values 0.1, 0.2, 0.3, where in the case of $r = 0$ this mode vanishes. Considering the $r = 0.1$ case (solid line), one can see that two complex conjugate roots appear in the kv_{1e} / ω_{pe} interval (0, 0.18), then these two roots disappear and two new real roots appear for $kv_{1e} > 0.18\omega_{pe}$. The corresponding imaginary parts for the modes appearing in Fig. 3 are shown in Fig. 4, where the solid line curve corresponds to the root that is presented in solid line in Fig. 3. The instability is about five times higher than that shown in Fig. 2 for the other unstable mode, and appears for values of k much lower (higher wavelength) than those for the other unstable mode. Increasing the r−value enhances the instability and blue shifts the maximum value.

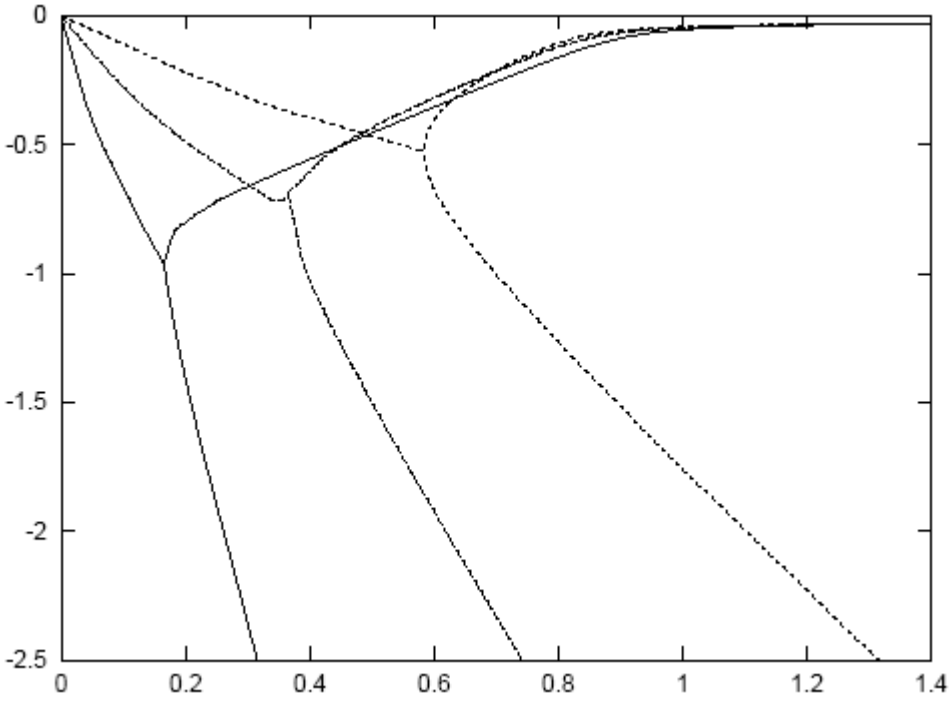

FIG. 3. Real part of the two new roots resulting from the solution of Eq.10. Unstable complex conjugate roots split into two real roots beyond some kv_{1e} / ω_{pe} value. Roots from left to right correspond to r = 0.1, 0.2, 0.3, respectively, where solid line corresponds to r = 0.1.

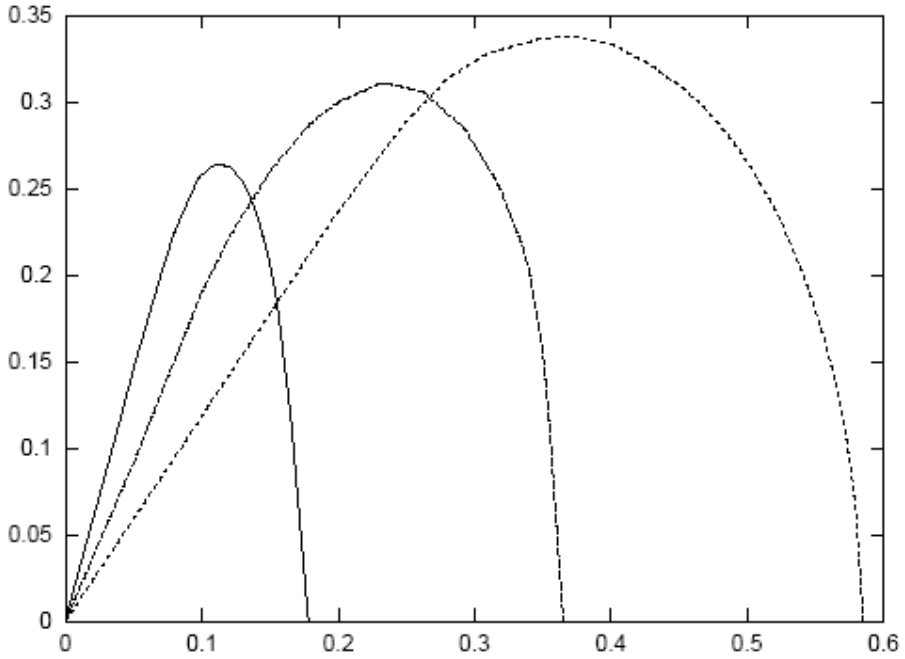

FIG. 4. Imaginary part of the unstable complex roots shown in Fig. 3, where complex roots have a cut−off at some kv_{1e}/ω_{pe} value. Peaks from left to right correspond to r =0.1, 0.2, 0.3, respectively.

In the rest of this section we will again consider hydrogen plasma and track the other modes of Eq. 10 shown in Fig. 1 and see the effect of introducing the new electron stream on this mode; the two real modes that start in Fig. 1 with ± 1 values are shown in Figs. 5 and 6 for values of r = 0, 0.1, 0.2, 0.3, where the solid line represents the case r = 0, i.e. the two−stream system. As can be seen, nothing much happens to the root starting with $\omega \approx +\omega_{pe}$ at $kv_{1e} = 0$, while the root that starts with $\omega \approx -\omega_{pe}$ at $kv_{1e} = 0$ changes from convergence to zero for higher kv_{1e} values in case of $r = 0$ to divergence as r increases. This shift down in the curves of Figs. 5 and 6 as r increases may be explained as a result of larger negative v_{2e} leading to this down shift.

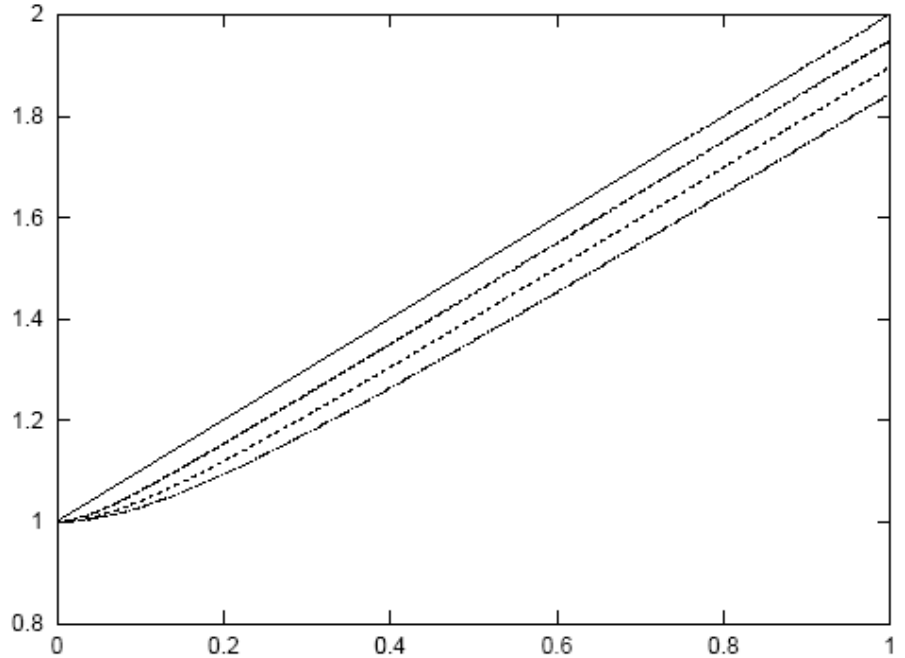

FIG. 5. Stable mode appearing in Fig. 1 for two−stream case (solid line with r =0), but here for three−stream case with r−values given by 0, 0.1, 0.2, 0.3, respectively.

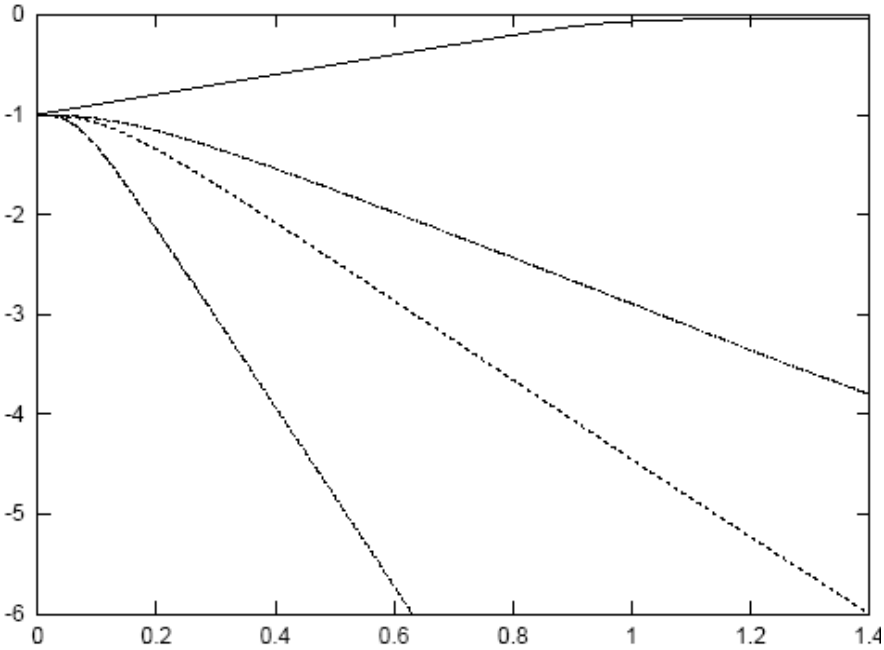

FIG. 6. Stable mode appearing in Fig. 1 for two−stream case (solid line with r = 0), but here for three−stream case with r−values given by 0, 0.1, 0.2, 0.3, respectively.

Fig. 7 shows the two complex conjugate roots that disappear at around $kv_{1e} \approx \omega_{pe}$, beyond which two new real roots appear instead (recall Fig. 1). The solid line represents the $r = 0$ case, i.e. the two−stream case, while the other curves represent the cases of r = 0.1, 0.2, 0.3, respectively. The instabilities of these roots are shown in Fig. 8, where, as in Fig. 7, the solid line corresponds to $r = 0$. Other curves correspond to r = 0.1, 0.2, 0.3, respectively. Different values of r don't affect the peak value of the growth rate but this peak does red shift as r increases.

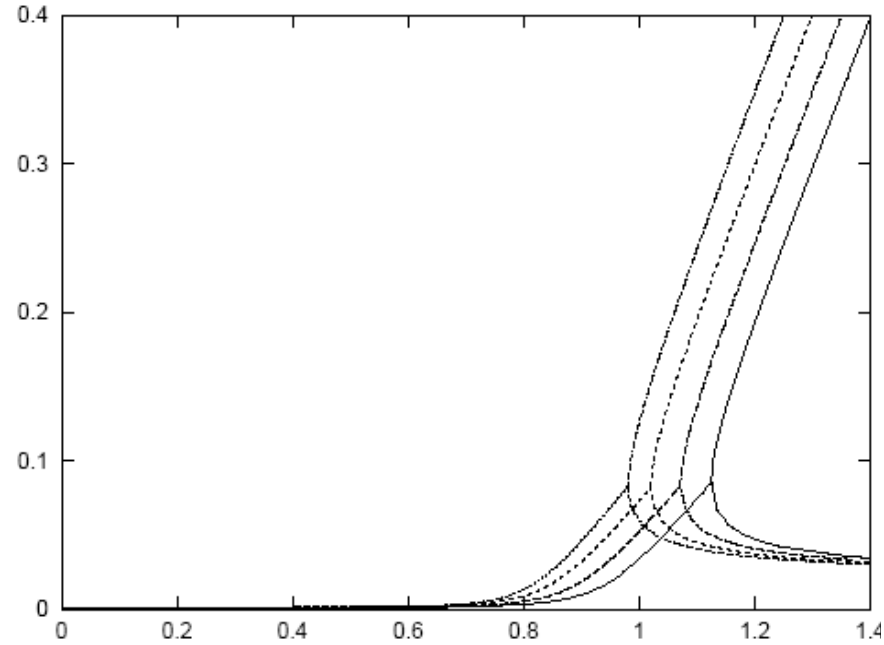

FIG. 7. Two roots appearing in Fig. 1 for two−stream case (solid line with r = 0), but here for the three−stream case with r−values given by 0, 0.1, 0.2, 0.3, respectively. Two unstable, complex conjugate roots split into two real roots beyond some kv_{1e} / ω_{pe} value.

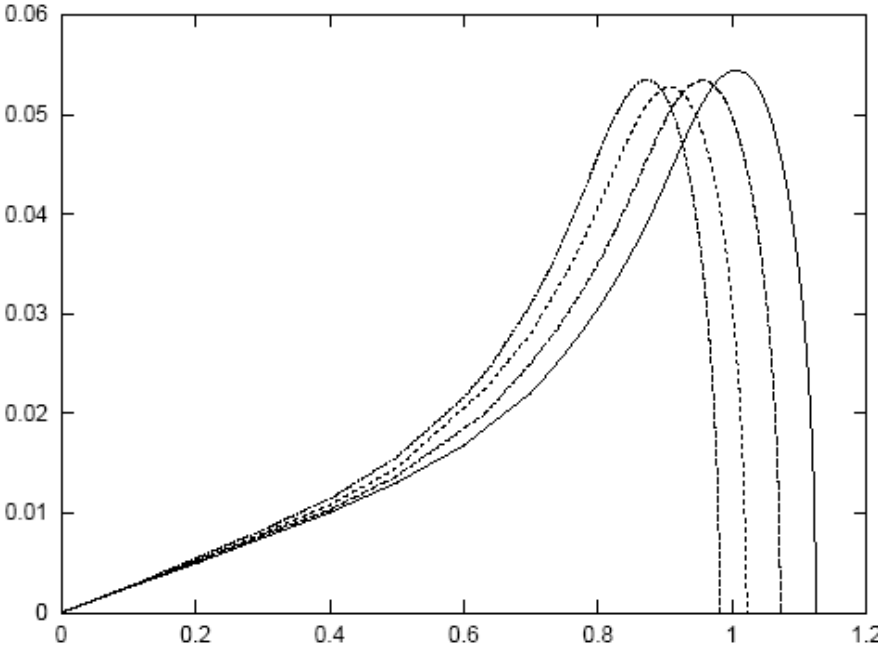

FIG. 8.. Imaginary part of the complex conjugate root of Fig. 7, where solid line represents the two−stream case, i.e. $r = 0$ and the rest of curves represent the $r = 0.1, 0.2, 0.3$ values, respectively.

For diagnostic purposes one can have a look at the "red−shift" of the peak of instability for the two unstable modes ($\Delta\gamma_m$) versus the r−value, where $\Delta\gamma_m$ is the difference in position of the peak value for some r−value and the position of the peak value for $r = 0$. Fig. 9 shows the result, where the solid line represents the red shift for the high instability mode. The relationship is not linear. For the first unstable mode appearing in both two and three stream cases, the red shift tends to a plateau as the r−value increases. For the highly unstable mode, appearing only in $r \neq 0$, the red shift decreases as the r−value increases.

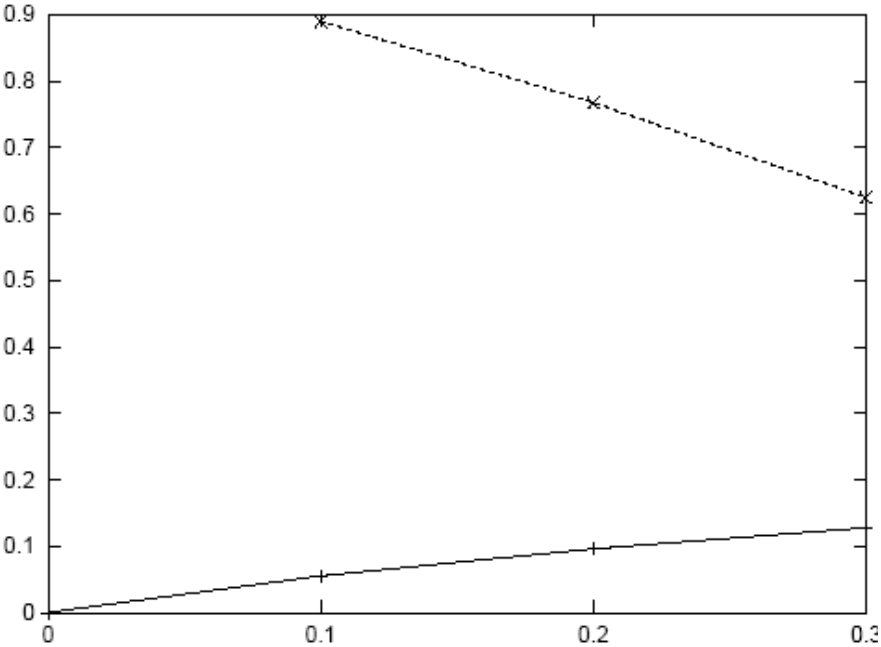

FIG. 9. Shift in position of maximum growth rate $\Delta\gamma_m$ versus r−value. Solid line represents unstable root appearing in two and three stream case. Dotted line represents the other, highly unstable mode appearing in the three−stream case, i.e. $r \neq 0$.

Conclusions

This paper summarizes our investigation on streaming plasma systems, namely e–i two–stream system and e–e–i three–stream system, where numerical solutions for the dispersion relations of the instabilities is considered. For $\varepsilon(k,\omega)=0$, Eqs. 6 and 10 represent the dispersion relations for the two cases, respectively. In this work the two dispersion relations are solved numerically, where the unstable modes are looked at in detail.

For the two–stream case, two complex conjugate roots corresponding to unstable modes were found. The peak value of the growth rate for this mode obtained from the numerical solution appears at $kv_{1e}=\omega_{pe}$ as expected from Eq.6. It is compared with those approximate values reported in literature, namely Eqs. 7 and 8. The numerical estimates of Fig. 2 show a maximum growth rate of $\gamma=0.055\omega_{pe}$, coinciding with that maximum of ref. [23] and showing an error of about 17% in the estimates of refs. [38, 39]. This is a good test for the validity of different approximate formulas widely used in literature.

Introducing a third species of electrons, drifting opposite to the first electron species, the ratio *r*, that represents the percentage of electrons in the second species with respect to the total number of electrons, is found to modify the instability and to give rise to a much more unstable new mode. The drift velocity of the second electron stream with respect to that of the first stream has been estimated such that the net current is zero, i.e. the relative velocity of the second electron species depends on the percentage number *r*.

The four modes, observed in the two–stream case, continue to appear in the three–stream case. For the unstable mode, seen in Fig. 2 of the two–stream case, the instability red shifts the peak slightly as the *r*–value increases, while its maximum doesn't change significantly. The most important result here is the appearance of a new unstable mode with a maximum growth rate of about five times that for the first unstable mode. This instability appears at much lower wavelengths compared to the unstable mode appearing in the two–stream case.

The appearance of this mode can be understood by comparing its frequency appearing in Fig. 3 with that of the other unstable mode shown in the solid line of Fig. 2 and in Fig. 7, where figures show a frequency of this mode close to the plasma frequency in the ion frame of reference. Such a high frequency/high phase speed wave can't interact easily with the heavy ions. In this case, neglecting the first term on the right hand side of Eq. 10, that represents ion contribution, leaves the system closely similar to a two–electron species system that gives a high frequency mode, like this one obtained in this work, with a maximum instability superior to that of the other mode appearing in the two stream and three–stream regime. The instability of such a two, counter streaming, electron gas can be referred to as the electron bi–stream instability.

References

[1]Krall, N.A. and Liewer, P.C., Phys. Rev. A, 4 (1971) 2094.

[2]Demchenko, V.V., Nucl. Fusion, 11 (1971) 245.

[3]Rosenbluth, M.N. and Rostocker, N., Phys. Fluids, 5 (1962) 776.

[4]Ishihara, O. and Hirose, A., Phys. Rev. Lett. 44 (1980) 1404.

[5]Gary, S.P., Phys. Fluids, 30 (1987) 2745.

[6]O'Neil, T.M. and Malmberg, J.H., Phys. Fluids, 11 (1968) 1754.

[7]Cairns, I.H., Phys. Fluids B, 1 (1989) 204.

[8]Lovelace, R.V. and Sudan, R.N., Phys. Rev. Lett. 27 (1971) 1256.

[9]Sato, T., Phys. Rev. Lett. 28 (1972) 732.

[10]Gary, S.P., "Theory of Space Plasma, Microinstabilities", (Cambridge Uni. Press, 1993).

[11]Hirosa, A., Plasma Phys. 20 (1978) 481.

[12]Gurnett, D.A., "Waves and instabilities in Physics of the Inner Heliosphere II", (Springer−Verlag, Berlin, 1991).

[13]Marsch, E., "Kinetic physics of the solar wind plasma, in Physics of the Inner Heliosphere II", (Springer−Verlag, Berlin, 1991).

[14]Marsch, E., J. Geophys. Res. 90 (1985) 6327.

[15]Gurnett, D.A., "Plasma waves and instabilities, in Collisionless Shocks in the Heliosphere": Review of Current Research, Geophysical Monograph 35, (American Geophysical Union, Washington DC, 1985).

[16]Neuffer, D. *et al.*, Nucl. Instr. Methods Phys. Res. A, 321, (1992) 1.

[17]Giovannozzi, M., Metral, E., Metral, G., Rumolo, G. and Zimmermann, F., Phys. Rev. ST Accel.. Beams, 6 (2003) 010101.

[18]Keil, E. and Zotter, B., CERN-ISH-TH/71-58, Technical report, (CERN, 1971).

[19]Laslett, L.J., sessler, A.M. and Moehl, D., Nucl. Instr. Methods Phys. Res. 121 (1974) 517.

[20]Rumolo, G., Bellodi, G., Ohmi, K. and Zimmermann, F., "Proc. of EPAC 2004", (Published by the European Physical Society Accelerator Group EPS-AG 1963-65).

[21]Zenkevich, P., Mustafin, N. and Boine-Frankenheim, O., "Proc. of ECLOUD 2002", (Yellow Report CERN, 2002-001).

[22]Zhang, S.Y. *et al*., Phys. Rev. ST, 8 (2005) 123201.

[23]Lapuerta, V. and Ahedo, E., Phys. Plas. 9 (2002) 1513.

[24]Ahedo, E. and Lapuerta, V., Phys. Plas. 8 (2001) 3873.

[25]Lapuerta, V. and Ahedo, E., Phys. Plas. 7 (2000) 2693.

[26]Lapuerta, V. and Ahedo, E., Phys. Plas. 9 (2002) 3236.

[27]Davidson, R.C. and Qin, H., Phys. Rev. ST Accel. Beams, 6 (2003) 104402.

[28]Bosch, R.A., Phys. Rev. ST Accel. Beams, 6 (2003) 074201.

[29]Blaskiewicz, M. *et al*., Phys. Rev. ST Accel. Beams, 6 (2003) 014203.

[30]Anderson, D. *et al.*, Phys. Rev. E, 65 (2002) 046417.

[31]Channell, P.J., Phys. Rev. ST Accel. Beams, 5 (2002) 114401.

[32]Haas, F., Manfredi, G. and Fexi, M., Phys. Rev. E, 62 (2000) 2763.

[33]Anderson, D. *et al*., Phys. Rev. E, 65 (2002) 046417.

[34]Ali, S. and Shukla, P.K., Eur. Phys. J. D, 41 (2007) 319.

[35] Ali, S. and Shukla, P.K., Phys. Plasmas, 15 (2008) 044503.

[36]Ren, H., Wu, Z.W., Cao, J. and Chu, P.K., J. Phys. A,: Math. Theo., 41 (2008) 115501.

[37]Ren, H., Wu, Z.W., Cao, J. and Chu, P.K., Phys. Plasmas, 15 (2008) 082103.

[38]Chen, F.F., "Introduction to Plasma Physics and Controlled Fusion", Vol. I, (Plenum Press, New York and London, 1985).

[39]Nicholson, D.R., "Introduction to Plasma Theory", (John Wiley and Sons, NY, 1983).